Journal of Engineering Science and Technology
Vol. 12, No. 4 (2017) 1022 - 1036
© School of Engineering, Taylor's University

NUMERICAL SIMULATION OF PH EFFECT ON COPPER ELECTRODEPOSITION INSIDE INSULATED TRENCH - PART I

WATHEQ NASER HUSSEIN

Babylon University, College of Engineering, Iraq
E-mail: wathq777@yahoo.com

Abstract

Current distribution of copper electrodeposition in a trench (at different flow conditions) was studied taking into consideration the effect of hydrogen evolution. Due to pH effect on solubility of Cu^{+2} ions and the feasibility to precipitate as hydroxides at high pH, thus the importance of such study was handled. The results showed that the deposition in general was non uniform along the lateral walls, the non-uniformity not affected by current or flow velocity. Velocity not affect H^+ concentration inside the trench and its value remained the same as that for the initial one meaning that Cu hydroxide precipitate was not possible.

Keywords: Current distribution, Modeling, Comsol, Electrodeposition, Copper, Trench.

1. Introduction

Copper electroplating from acidified copper sulfate is a classical technology [1], dating back to the early 1800's. Today, copper electrodeposition is a major plating processes with important applications in electronics (printed circuits, connectors), steel coating, and in electroforming. There are several types of plating baths used to electrodeposit copper which include acid copper, cyanide copper, and pyrophosphate systems [2]. Although all three systems can be found in use today, acid copper plating is the most common system used for copper electrodeposition. The main component of acid copper plating solution is $CuSO_4$ as a source for cupric ions and the H_2SO_4 acid plus some additives [3].

Complicated parts with crevices, trenches, slots, inner hollow diameters are widely used in some domestic demands and mainly in military application as well as a progressing electronic technology. In these fields acid copper plating baths

Nomenclatures

bc	Cathodic Tafel slope, V
Cb	Bulk concentration, mol/m^3
C_i	Concentration of ith species, mol/m^3
D_i	Diffusivity of ith species, m^2/s
F	Faraday constant, coulombs /mol
g	Gravity vector, m / s^2
I	Current density, A/m^2
i_0	Exchange current density, A/m^2
m	Mass flow rate, kg/s
N_i	Molar flux of ith species, mol/m^2.s
p	Pressure, kg /m s^2
R	Gas constant, 8.3 J/mol. K
R_I	Homogenous reaction rate, mol/m^2.s
T	Temperature, K
umi	Ion mobility of ith species, m^2/V.s
u	Velocity vector, m /s
V	Potential or voltage, V
z_i	Charge number of i-th species

Greek Symbols

μ	Viscosity, kg/ m.s
ρ	Density, kg /m^3
η	Overpotential, V

are used in limited extent since it lacks a perfect throwing power and sometimes they are used after some preliminary treatments [3] or with additives [4].

Many researchers [5, 6] dealt with filling trenches and holes with different aspect ratio in electronic industry but the problem of current distribution in this case is less in complexity compared to thin deposition of copper on inside walls due to design limitation and restrictions. Applied current in the practical electroplating baths has no unique value and it has an average one. Character of the deposits, its distribution, the current efficiency and the formation of the deposit all may depend on the current density [3, 7]. Stirring of the solution or the electrodes, agitation, mixing either by mechanical or by air bubbling all of them are means used in some baths to enhance mass transfer and improve the appearance of deposits [3, 7]. Low et al. [8] studied some parameters effect on potential and current distribution along the rotating cylinder electrode; they found that the local current density along the electrode is increased by increasing velocity or rotation of the electrode. Kim et al. [9] studied the effect of flow on copper electrowining using flat plates and they found that increasing velocity led to decreased overpotential owing to a smaller diffusion boundary layer thickness. Other factors have pronounced effects on copper electrodeposition even when the current below the limiting value, also the electrode kinetics have their own effects [10].

The evolution of hydrogen is an undesired side reaction, which competes the copper deposition reaction and therefore reduces the efficiency of deposition [11]. It depends on the potential it possesses to be evolved. Evolution of hydrogen with copper electrodeposition has two effects [12]; the first effect is a reduction of the

diffusion layer thickness and the increase of the limiting diffusion current density. The second effect concerns the morphology of the copper deposits due to the effect of hydrogen bubbles on the current density distribution hence on the growing electrode surface. One of the most important things in electrodeposition is the solubility-pH- range for the specified ion [13] and the stability of the solution. The pH has a pronounced effect on hydrogen evolution through its effect on the free Cu^{+2} ions in the solution which are the main source for electrodeposition where increasing pH leads to formation of cupric hydroxide products which leads to reduction in the concentration of Cu^{+2} free ions and preventing further deposition by accumulation on the surface and impair the deposits quality. In objects subjected to bad current distribution such as holes, trenches etc. there will be a chance for H ions concentration in acidic baths to be varied along the surfaces as well as the metal ions source, accordingly the solubility-ions should be taken into consideration for its important factor. The situation looks like a crevice corrosion where some ions and their distribution play a vital role. It was ascertained [14] that increasing pH and copper sulfate concentration micro-roughness decreases as a consequence of increasing copper transport number, that is, lowering concentration polarization has a beneficial effect on deposit microdistribution. Mathur et al. [15] found that by increasing the pH value in the range of his study has a pronounced effect on increasing copper electrodeposition current where they used ITO as a substrate. This fact –for Cu^{+2}-H^{+} codeposition- could not be touched when the solution volumes are large and the electrode sizes are small for a short time interval and for practical values of current densities but it has a pronounced effect if the electrodeposition taking place within the narrow holes or trenches at high reaction rate. As stated in above and in other studies [16-19] as well as to the best of our knowledge that these didn't deal with electrodeposition in such objects and there was no light shedding on the pH distribution inside the holes, trenches, etc. Due to the importance of such study especially in the military aspects, some parameters such as velocity, applied current, hydrogen ions concentration and their effect on current distribution were studied as well as checking the limit of pH variation values within the trench.

2. Formulation of Numerical Simulation

Tertiary current-potential distribution was analyzed in modeling the system under study. The primary distribution neglects all effects such as overpotentials and kinetic factors and interested in solution conductivity and geometrical factors [20]. The secondary current distribution takes into consideration the surface reaction and the related overpotential while the tertiary distribution deals with the effect of concentration variation near the electrode surface and the related mass transfer [20]. The specimen in this work is look like a tube opened from one end (trench) which opposite to the entering solution side and has dimensions of 1 cm×4 cm with an insulated external surface and internal surface made of copper and it is surrounded by two anodes having area of 1 cm×5 cm for each. The dimensions of the cell are 11 cm×10 cm. It is important to mention that one aspect ratio of the working electrode throughout this work is dealt with.

Steady state, laminar, incompressible flow has been considered and hence the following forms of the Navier–Stokes equations are applicable [21]

$$\nabla u = 0 \quad (1)$$

$$\rho u.\nabla u = \mu \nabla^2 u \nabla p + \rho g \quad (2)$$

In the ionic solution, transport of species I has the following expression called Nernst-Plank equation;

$$N_i = -D_i \nabla C_i - Z_i\, umiFC_i \nabla V + C_i u \quad (3)$$

$$(-D_i \nabla C_i - Z_i\, umiFC_i \nabla V) + u\nabla C_i = R_i \quad (4)$$

where *umi* is the ionic mobility which takes the form;

$$umi = D_i F/(RT) \quad (5)$$

Electroneutrality is also applicable inside the solution:

$$\sum C_i Z_i = 0 \quad (6)$$

In the absence of concentration gradient and zero velocity, Eq. (3) is reduced to the Laplace form of solution potential;

$$\nabla^2 V = 0 \quad (7)$$

Solution of Eq. (7) with appropriate boundary conditions leads to primary and secondary current distribution.

Laplace equation also can be applied to the concentration variation within the diffusion layer;

$$\nabla^2 C = 0 \quad (8)$$

For tertiary current distribution one can use the following equation:

$$i = i_0 C/Cb * exp(-\frac{\eta}{bc}) \quad (9)$$

which is a modified Tafel equation used to estimate the effect of mass transfer on current distribution. The model values are as follows:

$CuSO_4$ reference concentration is 188 g/l [3], copper exchange current density is 3.2×10^{-4} A/cm^2 [22], hydrogen exchange current density is 10^{-6} A/cm^2 [11], temperature is 25°C, average applied current i = 200 A/m^2 or 0.02A/cm^2 [3], pH = 4 [3], and Tafel slope for cathode is 45 mV [23].

It was assumed that inlet mass flow rate, *m*, is in the range of 0.1-0.5 kg/s (it is assumed that there was a pump circulates the electrolyte in the stated flow rates in order to create some convection effect.)

It is interesting to mention that Comsol 4.4 was used throughout this paper as a means for modelling and numerical solution.

3. Results and Discussion

Figure 1 represents the electroplating bath in which the working electrode is bounded by two inert anodes where the following electrochemical reaction takes place

$2H_2O=4H^++O_2+4e$

It is assumed that all anodic contributing effects are neglected. The tertiary current-potential distribution will be discussed. The working electrode is assumed to be insulated from outside and deposition take place on inside walls sections; L, R and B symbols were given to the left, right and bottom sections of the internal surfaces of trench respectively.

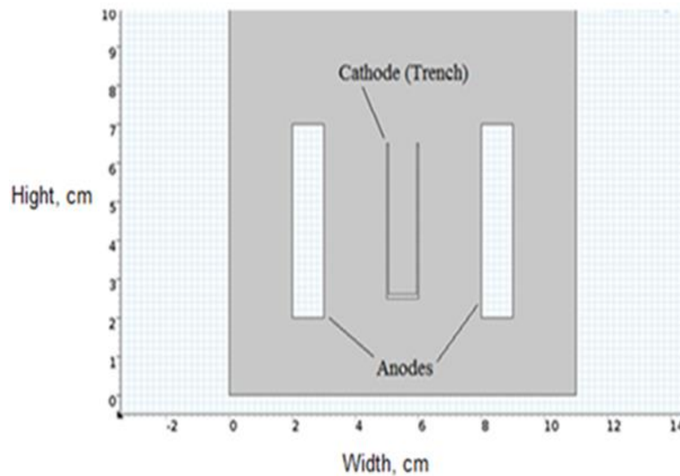

Fig. 1. The electroplating bath.

3.1. Relation between: copper deposition overpotential and local current

Figures 2(a) to (c) show the overpotential along the working electrode as stated by the symbols. From these figures, it is seen that at section B the overpotential is stable along the electrode and there is no variation, It is also indicated that the overpotential is decreased by increasing the applied current density [8].

The overpotentials at sections L and R are shown through Figs. 2(b) and 2(c) respectively and from those the same trend is seen for both; that is the overpotential has the same figure. The overpotential along section R and L are highly non uniform. Increasing applied current does not improve distribution but only leads to decreasing of overpotential.

From Fig. 3(a) the localized current distribution is shown, it is obvious that the local current is uniform slightly intensified at the half of section B due to convection. The variation of the applied current has no effect on the distribution but only it affects its intensity. The velocity has a very slight effect on local current density intensity which is attributed to aspect ratio of 1:4 that is the velocity components approximately reaches ~ zero inside trench (see Fig. 3(b) for comparison.) Therefore, it can be said that increasing velocity has no effect on distribution.

Approximately the current distribution on section R is the same as that of L where distribution on L is not shown due to similarity-that is the current distribution is highly non uniform along the electrode, Fig. 3(c), and the distinguish feature is that the applied current density variation does not affect the distribution. This trend of bad distribution is expected since the electrode is insulated and the only touching point with the solution is from its mouth. To do checking for the effect of velocity on such distribution Fig. 3(d) is constructed below. From Fig. 3(d), local current on R section does not affected by increasing velocity.

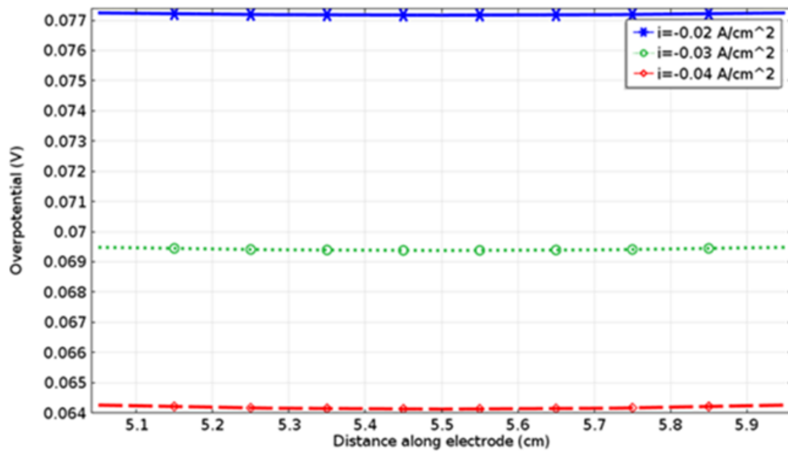

(a) Section B at m = 0.1 kg/s.

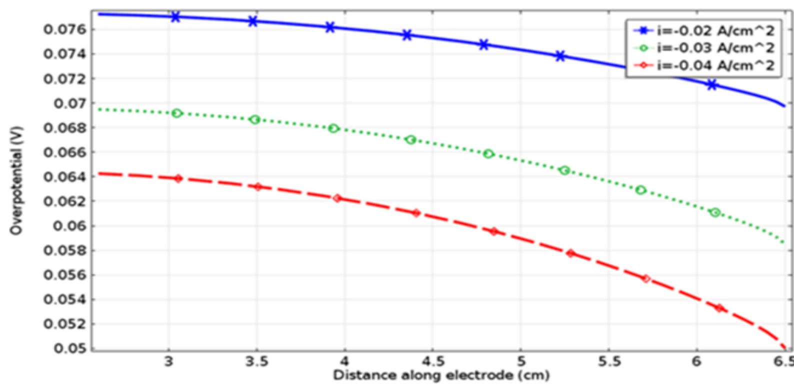

(b) Section L at m = 0.1 kg/s.

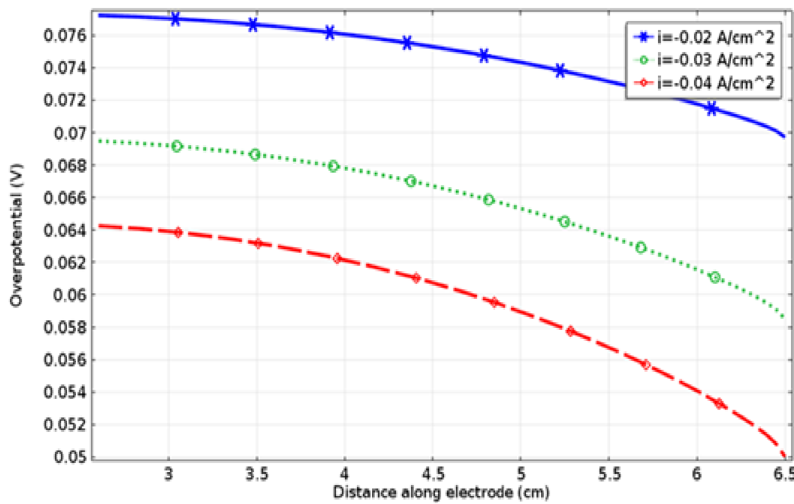

(c) Section R at m = 0.1 kg/s.

Fig. 2. Overpotential along the working electrode at different sections.

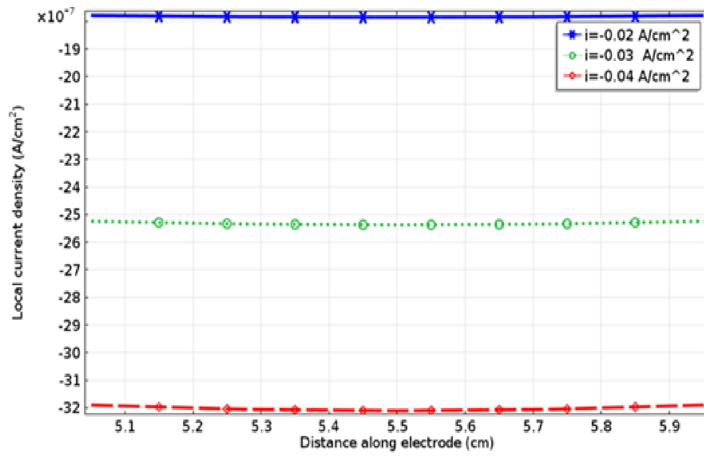

(a) Section B at *m* = 0.1 kg/s.

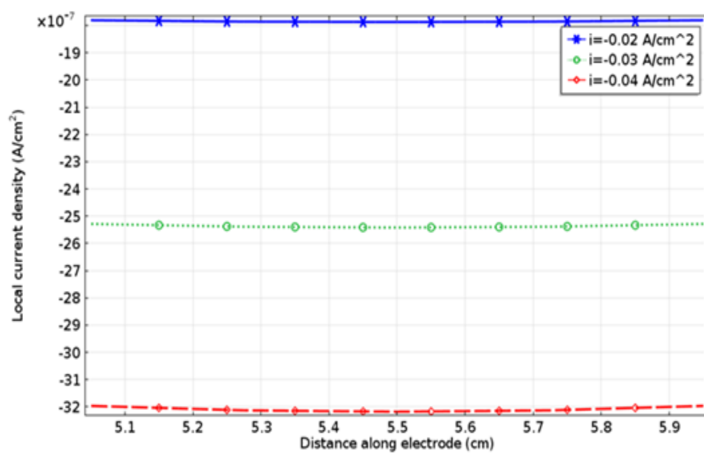

(b) Section B at *m* = 0.5 kg/s.

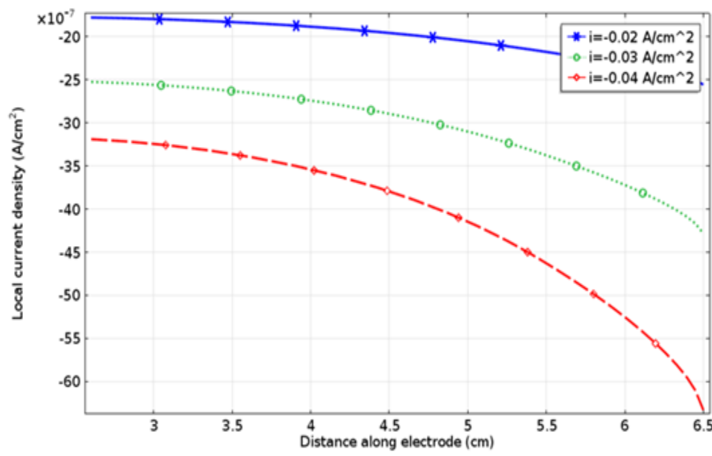

(c) Section R at m = 0.1 kg/s.

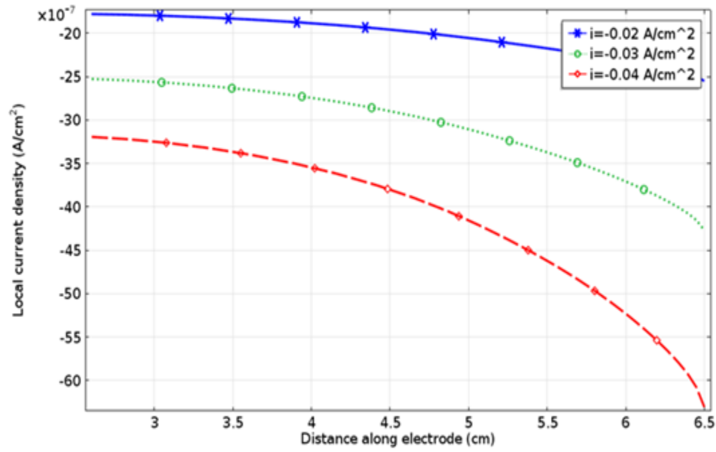

(d) Section R at *m* = 0.5 kg/s.

Fig. 3. Local current density along the electrode distance at different sections.

Due to poor effect of velocity on the distribution inside the trench -in general-where it has a very small values~0 on R and B - see Figs. 4(a) and 4(b)-, therefore, convection transport component approaching its minimum value at these sections, hence local current is minimized. It can be noted that at all the applied current values the velocity remained the same at the specified location along the cut line (in Fig. 4(a) cut line can be seen in the mid of the working electrode). This could indicate that there was no simulation of natural convection. It is interesting to note that section R delivers more current than B due to difference in path of current flowing between the two sections and the resulting ohmic losses.

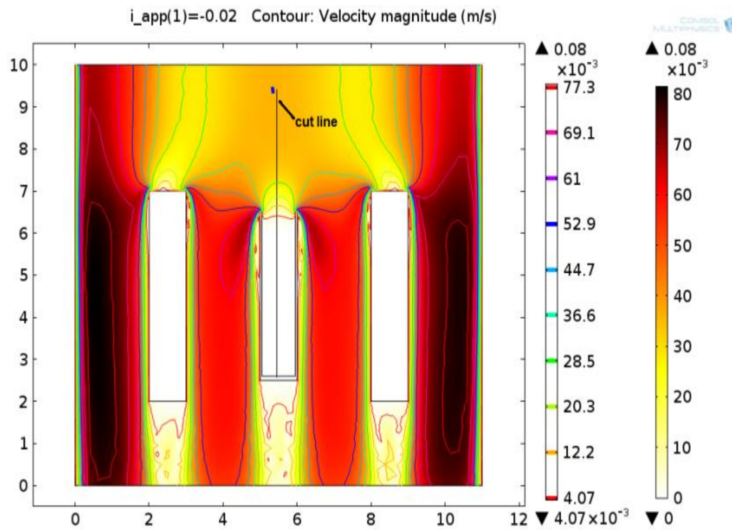

Fig. 4(a). Distribution of velocity around and inside the working electrode, at m=0.5 kg/s.

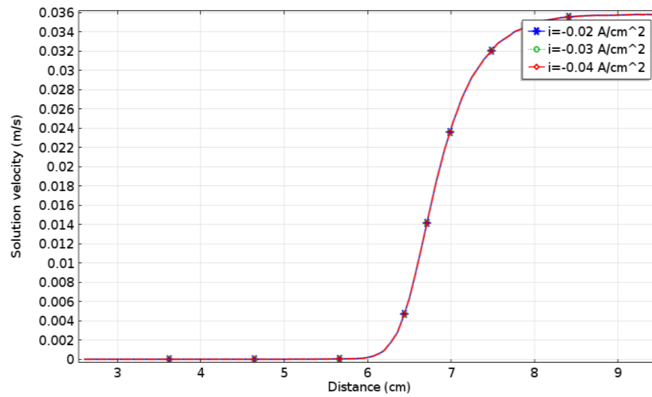

Fig. 4(b). Distribution of velocity along the cut line (shown in Fig. 4(a)) starting from B inside the trench towards the solution outside at m=0.5 kg/s.

3.2. Hydrogen ion H^+ concentration distribution

An important thing is to check the concentration distribution within the working electrode for the H^+ ions and their role in the process. Starting with hydrogen ion distribution at velocity corresponds to 0.1 kg/s, the result is as in Figs. 5(a) and 5(b).

By comparing Fig. 5(a) with Fig. 5(b), it is seen that velocity has a slightly reverse effect on surface concentration of H^+ at section B, i.e., concentration decreases as velocity increases due to corresponding slight increase in local current also it should be noted that the concentration distribution uniformity was not affected by applied current. The maximum H^+ concentration on the B section has a value of about 10.08×10^{-8} and 10.105×10^{-8} mol/cm^3 at both values of velocity which corresponds to a pH of about ~ 4. This value tells that the pH does not change from the initial one during the whole process (initial pH is 4) and Cu^{+2} ions has good solubility at this value of pH according to Palmer et al. [13]. It was found that H ion has a slight variation in its concentration along the cut line which extends from B section of the trench towards the solution outside noting that its concentration is increased towards the B section which could be attributed to the effect of migration component of the transfer process as indicated by Eq. (3) and the velocity variation has a neglected effect as can be seen in Figs. 5(c) and 5(d).

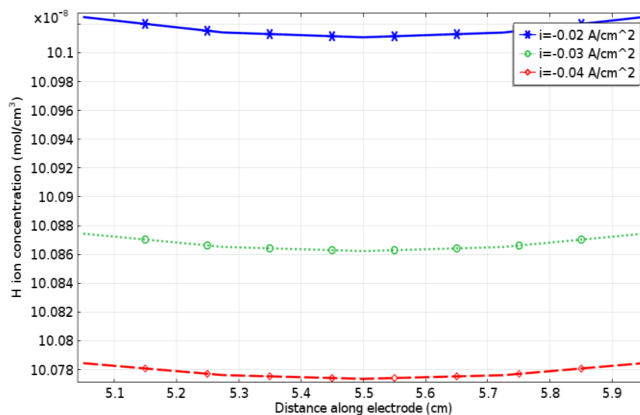

Fig. 5(a). H ion concentration distribution along section B at m=0.1 kg/s.

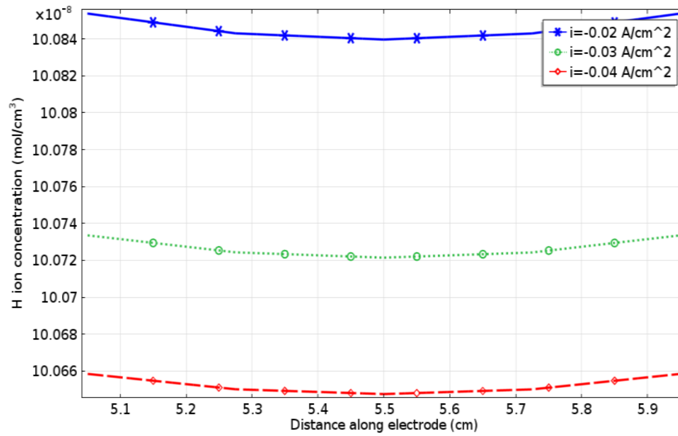

Fig. 5(b). H ion concentration distribution along section B at m=0.5 kg/s.

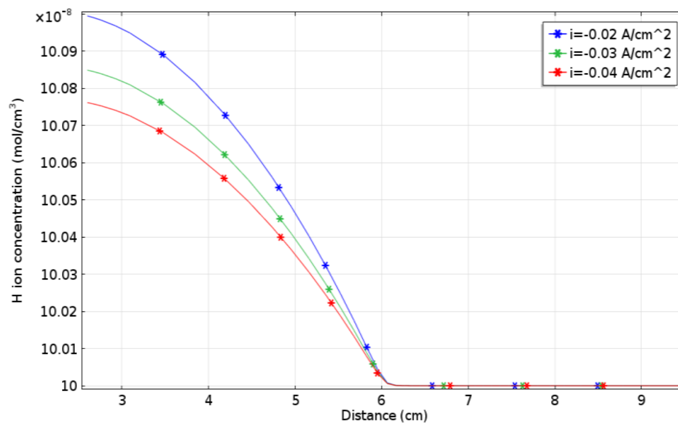

Fig. 5(c). H ion concentration along the cut line (shown in Fig. 4(a)) starting from B inside the trench towards the solution outside at m=0.1 kg/s.

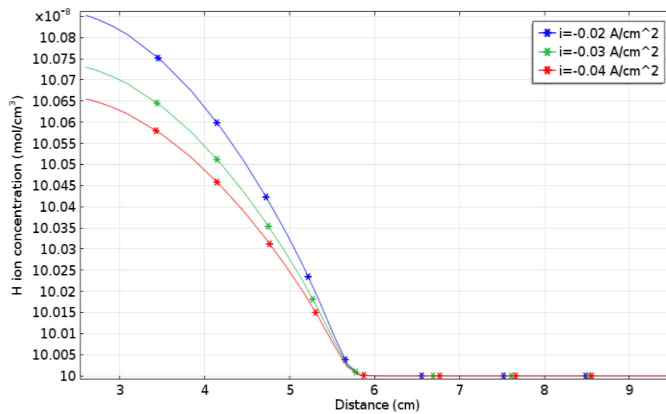

Fig. 5(d). H ion concentration along the cut line (shown in Fig. 4(a)) starting from B inside the trench towards the solution outside at m=0.5 kg/s.

3.3. Copper ion Cu^{+2} distribution and deposition efficiency

The efficiency of copper deposition as expected may exceed 100% and this is due to involvement of immersion deposition and the positive potential for copper deposition, Figures 6(a) to 6(e) show the copper deposition efficiency along sections B, R and L at two values of velocity. It is interesting to see that efficiency does not affected by velocity. As the applied current increases, the efficiency is slightly reduced which is attributed to depletion of copper ions as the overpotential decreases as well as the appearance H_2 evolution reaction.

Approximately the same efficiencies for copper deposition on both sections R and L as shown in Figs. 6(c) and 6(d), therefore, it is a case of symmetry and only section R will be checked at m=0.5 kg/s as illustrated in Fig. 6(e). By comparing Figs. 6(c) with 6(e), it can be say that there is no effect of changing velocity on the copper deposition efficiency on the lateral section. The values of the efficiency along the lateral sections are non-uniform where they are decreasing towards the bottom of the trench. As shown by those figures, by increasing the current, the efficiency is reduced due to two reasons:

- The first is the reduction in Cu^{+2}concentration to 1146 mol/m^3 at B section compared to that in the bulk where Cu^{+2} =1180 mol/m^3 as indicated by Fig. 6(f) (approximately the same trend for Cu^{+2} was seen for other sections; R and L, therefore; there is no need to show them),
- While the second is the hydrogen competing reaction; $2H^+ + 2e = H_2$which has overpotential values as can be seen in Fig. 7.

Comparing copper deposition overpotential Fig. 2(a) with hydrogen evolution overpotential Fig.7 it is very clear that copper will be deposited later or after the evolution of hydrogen which implies that the deposition efficiency is less than 100%, nevertheless the efficiency is about 100%. This discrepancy could be looked by returning back to the values of exchange current density values for Cu^{+2} deposition and H^{+2} evolution which are 3.2×10^{-4}[22] and 10^{-6} A/cm^2[11] respectively. Therefore, kinetic factors play an important role in determining the deposition efficiency.

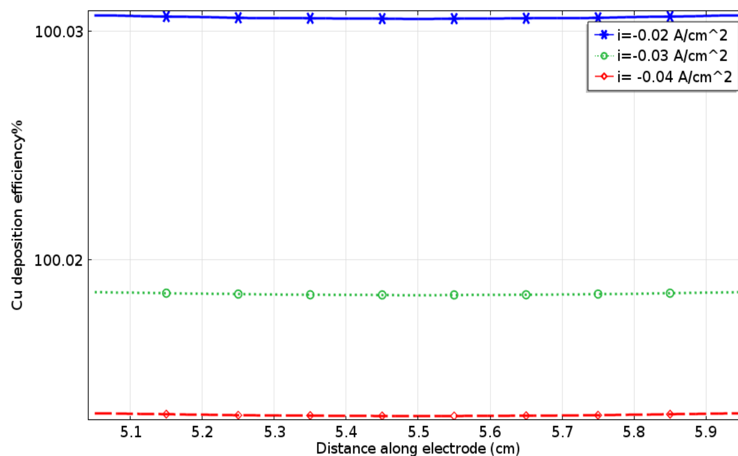

Fig. 6(a). Copper deposition efficiency versus distance along section B at m=0.1 kg/s.

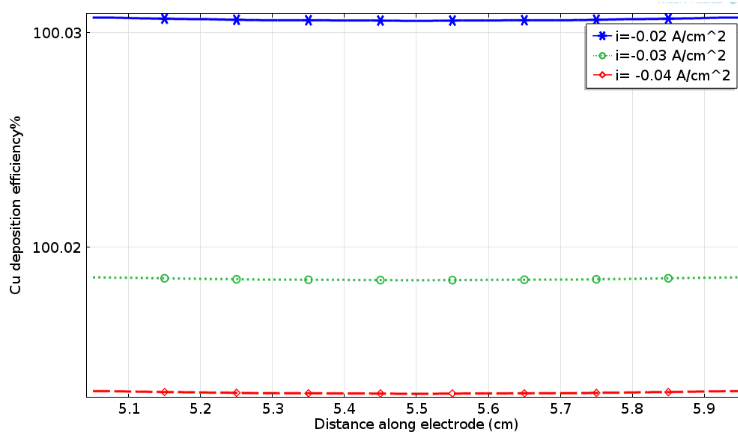

Fig. 6(b). Copper deposition efficiency versus distance along section B at m=0.5 kg/s.

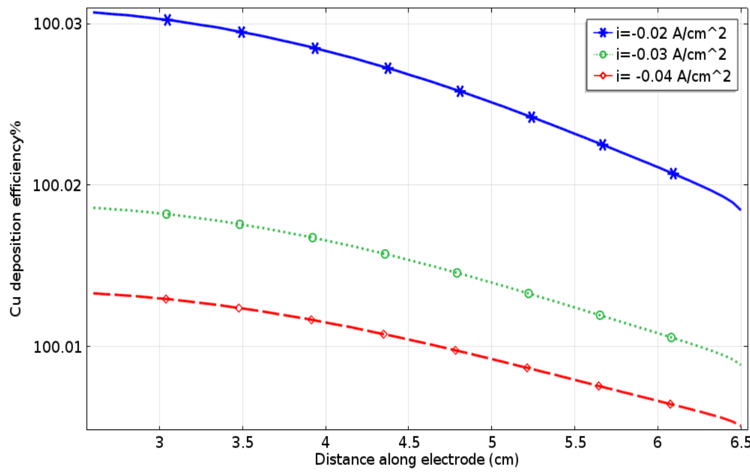

Fig. 6(c). Copper deposition efficiency versus distance along section R at m=0.1 kg/s.

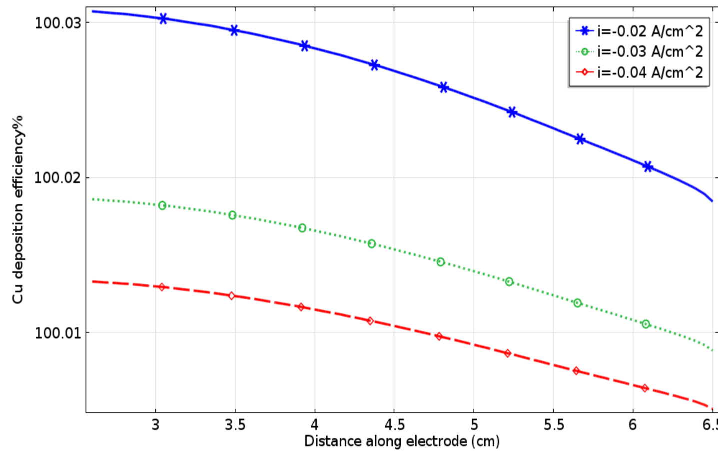

Fig. 6(d). Copper deposition efficiency versus distance along section L at m=0.1 kg/s.

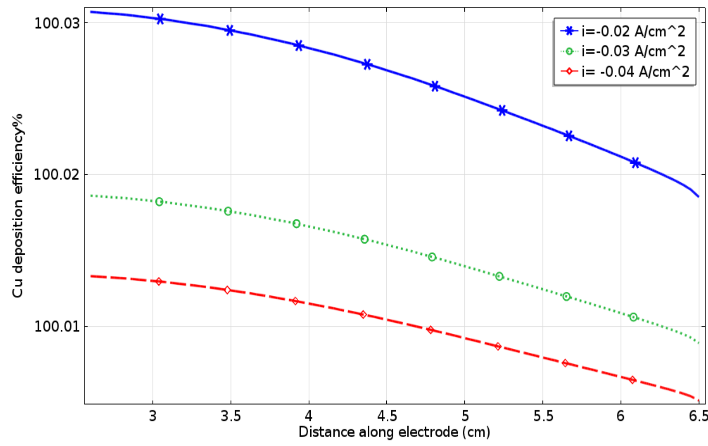

Fig. 6(e). Copper deposition efficiency versus distance along section R at m=0.5 kg/s.

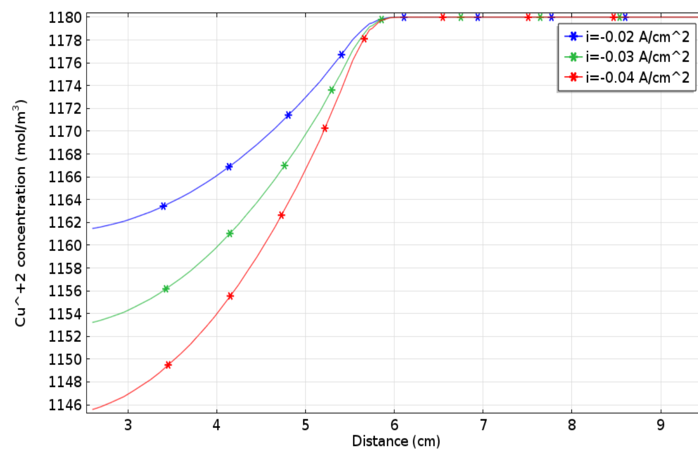

Fig. 6(f). Cu^{+2} ion concentration along the cut line (shown in Fig. 4(a)) starting from B inside the trench towards the solution outside at m=0.5 kg/s.

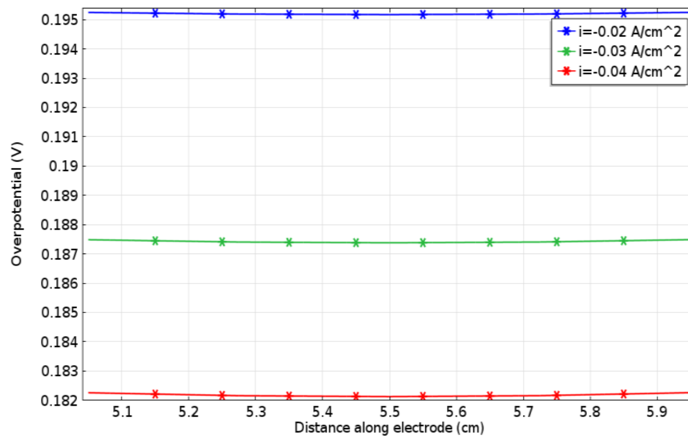

Fig. 7. Hydrogen evolution overpotential along the working electrode, section B at m = 0.1 kg/s.

4. Conclusions

From this work, the following conclusions were abstracted:

- Increasing of solution velocity has no effect on the uniformity of distribution; therefore, it is not important to force the solution to move for such shapes.
- Increasing the applied current increases the localized current and has no effect on current distribution.
- H ion concentration and its distribution do not affected by variation of velocity inside the trench or by the applied current.
- Throughout this study, there is no risk of copper precipitation due to solubility-pH effects inside the trench and the pH is still has the same value as in the beginning of the experiment.
- The deposition process of copper on the bottom side of the geometry used in this study has about 100% efficiency and does not affected by applied current or by variation of velocity.
- Kinetic factors such as exchange current density play an important role in determining the deposition efficiency.

5.Suggestions for Further Work

Unsteady state study could be addressed for the same system to check the Cu^{+2} concentration and the pH values with time as well as other parameters with making the outer surface of the working electrode conductive. Hopefully this suggestion will be the subject for part 2 holding the same title of this study.

References

1. Baker, B.C.; Pena, D.; Herrick, M.; Chowdhury, R.; Acosta, E.; Siimpson, C.R.; and Hamilton, G. (1999). *Eelectrochemical processing in Ulsi fabrication and semiconducter/metal deposition II*. Andricacos, P.C.; Alone P.; Searson, P.C.; Stickny J.L.; Reidsema-Simpson, C.; and Oleszek, G. (1999*). Proceedings of the International Symposium* (*Electrochemical Society Proceedings*), 25-40.
2. Robison, M.R. (2014). *Modeling and experimental validation of electroplating distribution in copper sulfate solutions*. MSc. Thesis. University of Utah, USA.
3. Lowenheim, F.A. (1978). *Electoplating.* Mc-Graw Hill.
4. Schlesinger, M.; and Paunovic, M. (2010). *Modern electroplating* (5th ed.). Wiley &Sons, Inc.
5. Dixit, P.; and Miaw, J. (2006). Aspect-ratio-dependent copper electrodeposition technique for very high aspect-ratio through-hole plating. *Journal of The Electrochemical Society*, 153(6), G552-G559.
6. Datta, M.; and Landolt, D. (2000). Fundamental aspects and applications of electrochemical microfabrication. *Electrochimica Acta,* 45(15-16), 2535-2558.
7. Kanani, N. (2004). *Electroplating, basic principles, processes and practice*. Elsevier Ltd.

8. Low, C.T.J.; Roberts, E.P.L.; and Walsh, F.C. (2007). Numerical simulation of the current, potential and concentration distributions along the cathode of a rotating cylinder Hull cell. *Electrochimica Acta*, 52(11), 3831-3840.
9. Kim, K.R.; Choi, S.Y.; Paek, S.; Park, J.Y.; Hwang, I.S.; and Jung, Y. (2013). Electrochemical hydrodynamics modeling approach for a copper electrowinning cell. *International Journal of Electrochemical Science,* 8(11), 12333-12347.
10. Landau, U.; D'Urso, J.J.; and Rear, D.R. (1999). Modeling the deposit thickness distribution in copper electroplating of semiconductor wafer interconnects. *Paper presented at the 195th Meeting of the Electrochemical Society.* Abstract No. 263, Seattle, WA.
11. Gabe, D.R. (1997). The role of hydrogen in metal electrodeposition processes. *Journal of Applied Electrochemistry,* 27(8), 908-915.
12. Djokic, S.S. (2010). *Electrodeposition: Theory and practice. Modern aspects of electrochemistry*, No 48. Springer-Verlag New York.
13. Palmer, D.A.; and Bénézeth, P. (2004). Solubility of copper oxides in water and steam. Proceedings of the *14th International Conference on the Properties of Water and Steam*, Kyoto, Japan, 491-496.
14. Vicenzo, A.; and Cavellotti, P.L. (2002). Copper electrodeposition from a pH 3 sulfate electrolyte. *Journal of Applied Electrochemistry*, 32(7), 743-753.
15. Mathur, J.; and Gupta, M. (2013). Effect of electrodeposition parameters on morphology of copper thin films. *The International Organization of Scientific Research (IOSR) Journal of Engineering*, 3(8), 55-61.
16. Kawai, S.; Fukunaka, Y. and Kida, S. (2009). Numerical simulation of ionic mass-transfer rates with natural convection in $CuSO_4$-H_2SO_4 solution I. Numerical study on the developments of secondary flow and stratification phenomena. *Journal of The Electrochemical Society*, 156(9), F99-F108.
17. Nikolić, N.D.; Branković, G.; Pavlović, M.G.; and Popov, K.I. (2008). The effect of hydrogen co-deposition on the morphology of copper electrodeposits. II. Correlation between the properties of electrolytic solutions and the quantity of evolved hydrogen. *Journal of Electroanalytical Chemistry*, 621(1), 13-21.
18. West, A.C.; Cheng, C.-C.; and Baker, B.C. (1998). Pulse reverse copper electrodeposition in high aspect ratio trenches and vias. *Journal of the Electrochemical Society*, 145(9), 3070-3074.
19. Gill, W.N.; Duquette, D.J.; and Varadarajana, D. (2001). Mass transfer models for the electrodeposition of copper with a buffering agent. *Journal of the Electrochemical Society*, 148(4), C289-C296.
20. Popov, K.I.; Živkovic, P.M.; and Nikolic, N.D. (2011). A mathematical model of the current density distribution in electrochemical cells. *Journal of Serbian Chemical Society,* 76(6), 805-822.
21. COSMOL (2016). Retrieved October 5, 2016, from www.comsol.com
22. Popov, K.I.; Djokic, S.S.; and Grgur, B.N. (2002). *Fundamental aspects of electrometallurgy.* Kluwer Academic Publisher, Springer US.
23. Madore, C.; Matlosz, M.; and Landolt, D. (1992). Experimental investigation of the primary and secondary current distribution in a rotating cylinder Hull cell. *Journal of Applied Electrochemistry*, 22(12), 1155-1160.